Synthesis of $TiO_2/WO_3/MnO_2$ Composites and High-Throughput Screening for Their Photoelectrical Properties

Zhijun Zou, Yuan Liu, Huayao Li, Yichuan Liao, and Changsheng Xie*

State Key Laboratory of Material Processing and Die & Mould Technology, Nanomaterial and Smart Sensor Research Laboratory, Department of Materials Science and Engineering, Huazhong University of Science and Technology, Wuhan 430074, PR China

Received January 19, 2010

On the basis of the idea of equilateral ingredient triangle, a material library of the $TiO_2/WO_3/MnO_2$ composite material system was designed, which consisted of 66 ingredient points. Each point in the library corresponded with a device. To fabricate the device, the technology of screen printing was used. The pastes which were suitable for this technology were prepared by ball milling. After we printed the pastes onto the alumina substrate which had been preprinted with Au interdigital electrodes, these printed samples were sintered at 550 °C for 2 h in air. The photocurrent of each device under different light sources was measured respectively using a high-throughput screening system. The largest photocurrent was observed when the mole ratio of TiO_2/WO_3 was 2/8 in the composite system. X-ray diffraction (XRD) was used to investigate the phase structure of the powder which had excellent photoelectric response.

1. Introduction

Ever since Fujishima and Honda in 1972 reported that TiO_2 as photoelectrode could split water under UV-light irradiation,[1] lots of researchers from material science, chemistry, and physics have paid much attention to the investigation of solar energy conversion and environmental purification with semiconductor-based materials.[2−5] Among them, photocatalytic degradation and elimination of organic contaminants become one of the most active research directions.

Currently, the studies of modification of a semiconductor have been researched intensively for organic pollutant degradation in both liquid and gas-phase conditions.[6−12] Generally speaking, the modification systems often showed a higher degradation rate as well as the increased extent of degradation. Nevertheless, few efficient semiconductor material systems have been found to be used in practice under visible light. Therefore, to increase the conversion efficiency and utilization rate of solar energy, the development of new semiconductor materials which exhibit high photocatalytic activity under visible light irradiation is needed.

However, developing new semiconductor material is not a simple process which can be carried out smoothly and expeditiously. Traditionally, in the selection and optimization of new materials, people often confine their thoughts to the way of trying, which plunges them into the pattern of "attempt−fail−try again".[13,14] As there are so many combinations of different mixed oxides in the case of a ternary oxide, this traditional method of discovery and optimization of new materials always consumes tremendous amounts of time and project cost but without any substantial progress.[15] Thus, to accelerate the screening of semiconductor materials, a time-saving, simple, and convenient method for their synthesis and characterization needs to be applied.

The method of combinational material science is a suitable way to solve the problem above, which can improve the overall efficiency of testing and screening for new semiconductor material of a system. Meanwhile, this method ensures the same condition and eliminates the human error greatly. Furthermore, it increases the probability of discovering new materials with an advantage of huge numbers.[16,17]

In our experiment, a material library of $TiO_2/WO_3/MnO_2$ composite system which is based on the idea of equilateral ingredient triangle of the ternary-phase diagram (described in the Experimental Section) with various mole ratios was designed, and the corresponding composite material pastes were synthesized by ball milling on a large scale. Owing to it could guarantee the contact between the electrode and materials layer favorably, the technology of screen printing was used to fabricate the flat-plate type devices using the as-prepared pastes. As one of the most important parameters for evaluation of the separation of the photoexcited electron and hole within the semiconductor materials, photoelectrical properties measurement was selected to evaluate the light response capability of the composite system, which has a promising practical application in degradation of organic contaminant under visible light and gas-phase condition. This is the significant difference to the conventional work provided by Dai and his co-workers, whom successfully designed and screened several triangle catalyst libraries for evaluation of the photodegradation activities of semiconductor catalyst.[18−20] During the testing, a high-throughput screening platform for the photocurrent measurement of the semiconductor was used. Here, the application of the combinatorial materials science for screening the photoelectrical properties of the

* Corresponding author. Tel: +86-27-8755-6544. Fax: +86-27-8754-3778. E-mail: csxie@mail.hust.edu.cn.

10.1021/cc1000117
Published on Web 03/12/2010

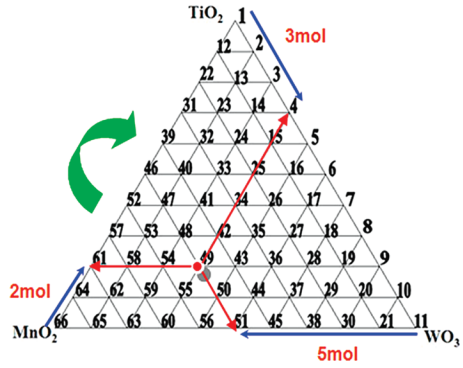

Figure 1. Material library design for 66 ingredient points. Point 49 was chose as an example to describe the mole ratio of each point for $TiO_2/WO_3/MnO_2$ " Ingredient triangle ". The mol ratio of $TiO_2/WO_3/MnO_2$ for point 49 is 2:3:5.

semiconductor materials under gas-phase condition is the biggest innovation of our research, which has great significance for the selection and research of visible-light-responsive semiconductor materials for photoelectrocatalysis and photocatalysis.

2. Experimental Section

2.1. Design of Material Library. On the basis of the idea of equilateral ingredient triangle of the ternary-phase diagram, a material library was designed (Figure 1), we named it "Ingredient Triangle", which consisted of 66 ingredient points. Of course, according to the idea of equilateral ingredient triangle, more ingredient points of an "Ingredient Triangle" can be designed. TiO_2, WO_3 and MnO_2 were chosen as the vertex material of the triangle. The mass of each point was 20 g. Here, point 49 was used as an example to describe their mole ratio of the ingredient point. The clockwise direction is defined as the positive direction, and 10 mol per point is supposed, according to the equilateral ingredient triangle, then the mol ratio of $TiO_2/WO_3/MnO_2$ for the point 49 is 2:3:5. The detail corresponding device number and mole ratio of each point were displayed in Table 1.

As for the selection of the three kinds of semiconductor materials, several reasons were considered. First, taking into account its relatively strong photocatalytic activity, biological and chemical stability, nontoxicity, low price, and long-term stability life against photocorrosion and chemical corrosion, TiO_2 was selected, which has been widely used in the fields of photocatalysis[21,22] and photoelectrocatalysis[23,24] for environmental purification. Second, WO_3 was chosen, due to it having a smaller band gap of 2.8 eV which can absorb both ultraviolet and visible light. Although it usually exhibited much lower photocatalysis activity using UV radiation compared with TiO_2, it was also concerned widely in the photocatalysis fields.[25,26] Finally, considering the energy band gap, MnO_2 was selected, as the band gap of MnO_2 was only 0.25 eV. Theoretically, it could absorb the light of infrared area. Except for this, the price of MnO_2 was inexpensive, and it is nontoxic. In addition, lots of literature about TiO_2 coupled with WO_3 or MnO_2 as a photocatalyst for degradation organic contaminants using different light source were reported.[27−29]

In brief, three kinds of materials, TiO_2, WO_3, and MnO_2 had been reported extensively as photocatalyst materials in degradation of organic pollutants under a different light source. Simultaneously, a band gap gradient formed among the energy band gap of $TiO_2/WO_3/MnO_2$; hence, the composite system might realize the total response to the solar spectrum. What is important? To our knowledge, the study of the photoelectric properties of a composite system which consisted of three kinds of semiconductors have been reported scarcely.

2.2. Samples Preparation. TiO_2 (100% anatase), WO_3, MnO_2 and other chemicals used in the experiment were of analytically pure grade. All of them were used as received without any pretreatment.

There are many methods to prepare semiconductor photoelectrodes, e.g., sol−gel, sputter deposition, etc. However, few works are reported to investigate the photocatalyst spreading on electrode by screen printing technique which was used under gas-phase condition. In this experiment, the synthesis of $TiO_2/WO_3/MnO_2$ composites was carried out in a QM-3SP04 ball miller (Nanjing University Instrument Factory, China). The typical process of the preparation for pastes was as follows. According to the ingredient triangles, the quality of the $TiO_2/WO_3/MnO_2$ powder of each point was taken (20 g at each point), and then, the powder and a certain amount of organic solvent (composed of terpineol, butyl carbitol, ethyl-cellulose, span 85 and di-*n*-butyl phthalate) were put into the agate ball milling tank in a mass ratio of 1 to 10 between the powder and agate ball. Organic solvent was used mainly as a thickening agent and a rheological agent for screen printing. After ball milling for 4 h at the speed of 300 rpm, the suitable pastes used for the process of screen printing were obtained. The pastes were collected and kept individually in the refrigerator for the next process. In a few words, the principal purpose of ball-milling was to mix the powder and gain the pastes which were suitable completely for screen printing.

$TiO_2/WO_3/MnO_2$ gas-phase photoelectrical flat-plate type devices were prepared by a screen printing technique, and the design parameters of the device were showed in Figure 2. By screen printing, the paste was printed onto the Au interdigital electrode which was preprinted on the alumina substrate; the thickness of each film was 10 μm which could be controlled by the screen printing machine. Then, the samples were dried for 30 min at 80 °C in an oven. After drying, in order to eliminate the organic solvent, these samples were heat treated successively for 30 min at 250 °C. In the end, the printed samples were transferred into the furnace and sintered at 550 °C for 2 h in air.

Following the above procedures, the fundamental flat-plate type device was obtained. This approach ensured the thickness of the film consistency, and the film could not fall off easily. To gain the entire device which was convenient for photoelectrical properties measurement, we needed to connect the Au electrode with the Au pedestal by a Gold Wire Bonder. The final devices that we applied to measure were shown in Figure 3.

Table 1. Mole Ratio and Device Number for Each Ingredient Point

ingredient (device) number	TiO_2:WO_3:MnO_2 (mol ratio)	ingredient (device) number	TiO_2:WO_3:MnO_2 (mol ratio)	ingredient (device) number	TiO_2:WO_3:MnO_2 (mol ratio)
1	10:0:0	23	7:1:2	45	0:6:4
2	9:1:0	24	6:2:2	46	5:0:5
3	8:2:0	25	5:3:2	47	4:1:5
4	7:3:0	26	4:4:2	48	3:2:5
5	6:4:0	27	3:5:2	49	2:3:5
6	5:5:0	28	2:6:2	50	1:4:5
7	4:6:0	29	1:7:2	51	0:5:5
8	3:7:0	30	0:8:2	52	4:0:6
9	2:8:0	31	7:0:3	53	3:1:6
10	1:9:0	32	6:1:3	54	2:2:6
11	0:10:0	33	5:2:3	55	1:3:6
12	9:0:1	34	4:3:3	56	0:4:6
13	8:1:1	35	3:4:3	57	3:0:7
14	7:2:1	36	2:5:3	58	2:1:7
15	6:3:1	37	1:6:3	59	1:2:7
16	5:4:1	38	0:7:3	60	0:3:7
17	4:5:1	39	6:0:4	61	2:0:8
18	3:6:1	40	5:1:4	62	1:1:8
19	2:7:1	41	4:2:4	63	0:2:8
20	1:8:1	42	3:3:4	64	1:0:9
21	0:9:1	43	2:4:4	65	0:1:9
22	8:0:2	44	1:5:4	66	0:0:10

2.3. High-Throughput Screening for the Photoelectrical Properties of $TiO_2/WO_3/MnO_2$ Composites and Characterization Methods. Due to the photocatalytic activity relying intensively on the type of contaminant and photocatalyst, the process of degradation of organic contaminant using photoelectrocatalysis was relatively difficult and time-consuming, which was not conducive to the high-throughput screening of the fundamental properties of the selected materials. Therefore, as one of the most important parameters for evaluation of the separation of the photogenerated electron and hole within the semiconductor materials, photocurrent measurement was selected to evaluate the response capability of the composite system for different light sources. Since it is supposed that the light response of the as-selected semiconductors could be verified in photoelectrical properties measurement,[30] it would be more efficient and could provide guidance for further investigation of the photocatalytic activity.

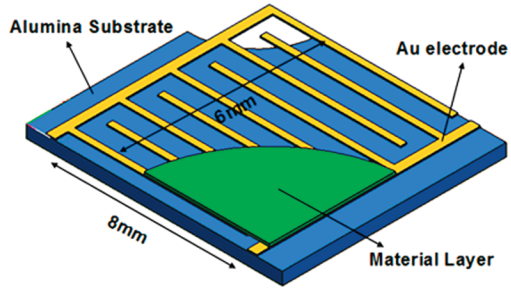

Figure 2. Schematic diagram of the flat-type device for photoelectrical property measurement.

Figure 3. Photograph of the 66 devices being prepared for high-throughput screening.

To measure the photocurrent of each device in the material library, a high-throughput screening platform (as shown in Figure 4) was used in this procedure, which was developed independently by our laboratory. One of the most significant features of the testing platform was that the photocurrent of 16 devices could be evaluated quickly and conveniently each time, and it avoided one device may affect other devices during the measurement. The testing phototcurrent range of the platform was $10^{-8}-10^{-3}$ A.

In the experiment, we selected four different light sources, which were white (400−800 nm), ultraviolet (365 nm), blue (475 nm), and green (525 nm). All of them were LED array light source (Shenzhen Ti-Times Co.). A bias voltage of 0.2

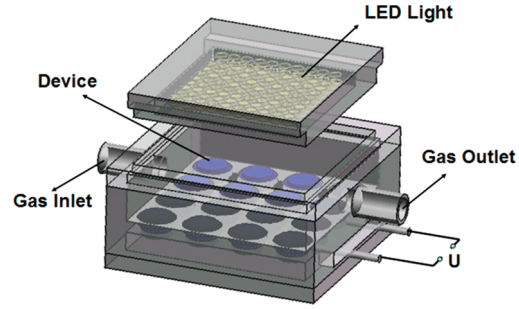

Figure 4. Schematic diagram of the testing chamber of the high-throughput screening platform.

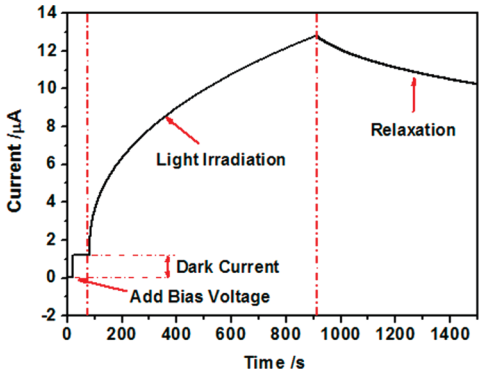

Figure 5. Photocurrent−time testing curve of device 9 (TiO_2/WO_3 = 2:8) using the high-throughput screening platform under 80 W/m^2 blue LED illumination adding 0.2 V bias voltage in dry air.

V was used to separate the photogenerated electron and hole. With the testing platform, the photocurrent could be acquired from each device when it was exposed to light illumination, and by exchanging the light source, a different photocurrent could be obtained.

To obtain the precise data of the phase composition of the corresponding powder of the device which exhibited remarkable response, an X-ray diffractometer (X'Pert PRO PANalytical B.V.) was applied using graphite monochromatic with Cu Kα1 radiation in the 2θ range from 20 to 60°.

3. Results and Discussion

3.1. Typical Testing Curve of High-Throughput Platform. According to the features of the design for the devices, the photocurrents of all the devices were measured. Figure 5 showed the photocurrent−time testing curve of device 9 (TiO_2/WO_3 = 2:8) using the high-throughput screening platform under 80 W/m^2 blue LED illumination adding 0.2 V bias voltage in dry air. As can be seen from the figure, the whole testing process could be divided into three main stages.

First, the bias voltage was applied (20−80 s), which was to force the free electrons within the semiconductor materials to move directionally. During this process, a dark current formed which could be detected in the external circuit. This stage exhibited the conductivity properties of the semiconductor materials in the dark.

Second, the light source was turned on (80−910 s). When the devices were exposed to the light source, the photogenerated electron−hole pairs formed. With the increase of the carrier inside the material, the current in the circuit increased rapidly. By means of data acquiring using the data acquisition card (PCI-6225, National Instrument Co.) which was performed by LabVIEW in the testing platform, the instantaneous current in the circuit could be obtained easily and expediently. Here, the applied bias voltage improved the charge separation and reduced unproductive recombination processes.

Third, the light source was turned off (910−1600 s). Due to the large number of carriers within the semiconductor materials, electron and hole would be recombined quickly after the stop of light irradiation. The direct result was that the testing current in the circuit was reduced rapidly as the fast decrease of the photogenerated carriers inside the material.

3.2. Overall Description of the Photoelectrical Properties of the Devices. Through measurement, we obtained the photoelectric response curve of all the 66 devices using the high-throughput screening platform. From the testing results, we found that many devices showed remarkable responses under different light source irradiation near the corner of WO_3, while, on the other two corners, TiO_2 and MnO_2, no obvious response was observed under any light irradiation.

Figure 6 showed the amplitudes of the photoelectric responses for all the 66 devices by application of a bias voltage of 0.2 V under white, ultraviolet, blue, and green light sources, respectively. These amplitudes were collected from the second stage of light irradiation. As can be seen from the figure, compared with other devices, device 9, which the mole ratio of TiO_2 to WO_3 is 2 to 8, showed a quite high photoelectric response both under ultraviolet and other light sources, and in them, one of the most special features for these results was that device 9 had response to green light; although the response amplitude was low, to our knowledge, similar results hadn't been reported in the literature up to now.

The material system for device 9 was TiO_2/WO_3, compared with device 1 and device 66 which was prepared separately by pure TiO_2 and WO_3 powders. It had a large response under the same light source and bias voltage. In a sense, this composite system expanded the scope of the absorption spectrum, which was also one of the main purposes why we designed this material system. X-ray diffraction (XRD) was used to investigate the phase structure of the powder for device 9 (Figure 7); the powder was prepared using the as-prepared paste, and the sintering process for it was the same with the material layer of the testing device. From the XRD analysis, there were just TiO_2 and WO_3 phases; a new phase was not formed during the process of ball-milling and sintering.

Due to the obvious difference from other devices, for device 9, we listed it separately to compare and discuss the unit power of photocurrent amplitude when it was exposed to ultraviolet, blue, green, and white (Figure 8a). From the figure, we could observe clearly that the response capability of device 9 for the three kinds of light under the same bias voltage was ultraviolet > blue > green. This result has showed the composite response to blue light, even green light, which means the composite can utilize the solar light. Although the composite has less response to the green light, it enlarges the response range compared to the single phase. The spectral characteristic of white light was shown in Figure 8b; two main peak values were observed from 440 nm to 580 nm, which displayed that the white light was mainly composed of blue and green.

It is obvious that the larger the photocurrent in the circuit, the more are the separation and transfer of the photogenerated electrons and holes within the semiconductor when the different material systems are measured under the same light source irradiation and bias voltage. In this experiment, the photoelectric response amplitude of device 9 was the largest

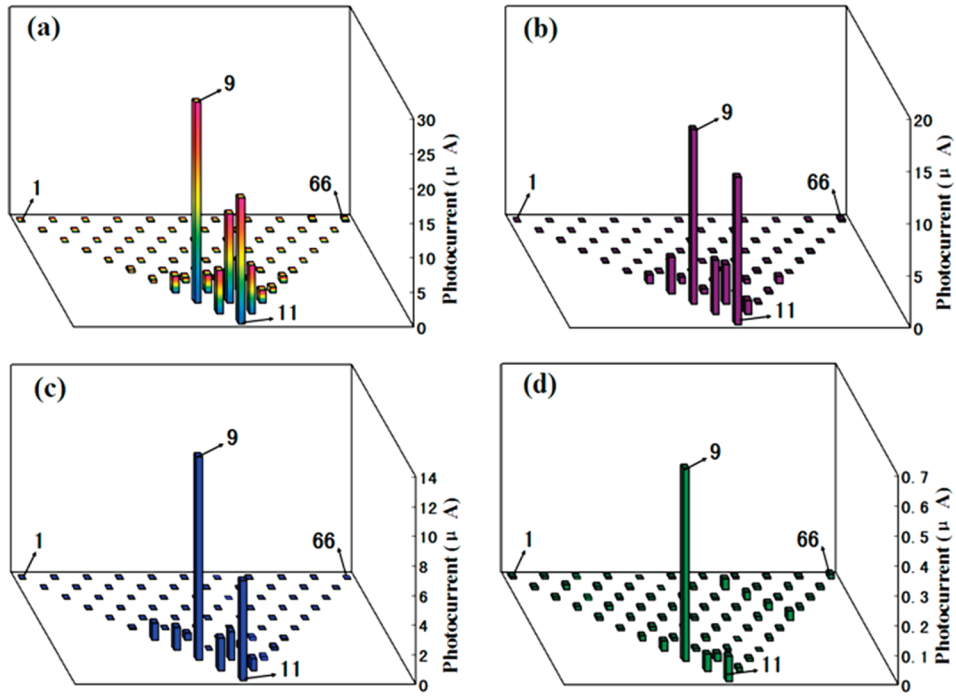

Figure 6. Photocurrent mapping of the different mole ratio $TiO_2/WO_3/MnO_2$ composites. Each point corresponding with a device. The devices were prepared through screen printing and sintering at 550 °C for 2 h. Testing environment: room temperature, 25 °C; humidity, <15% RH; applied potential, 0.2 V. Light source: (a) white (400−80 nm, 355 W/m^2); (b) ultraviolet (365 nm, 36 W/m^2); (c) blue (475 nm, 80.8W/m^2); (d) green (525 nm, 130W/m^2).

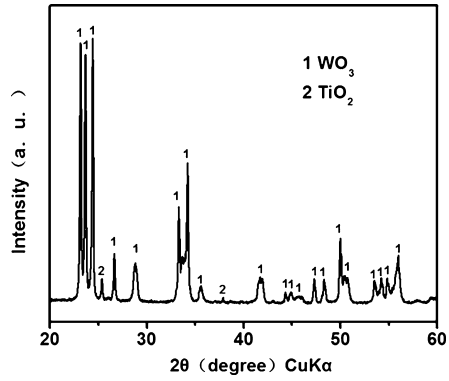

Figure 7. X-ray diffraction pattern of the powder of device 9 (TiO_2/WO_3 = 2:8).

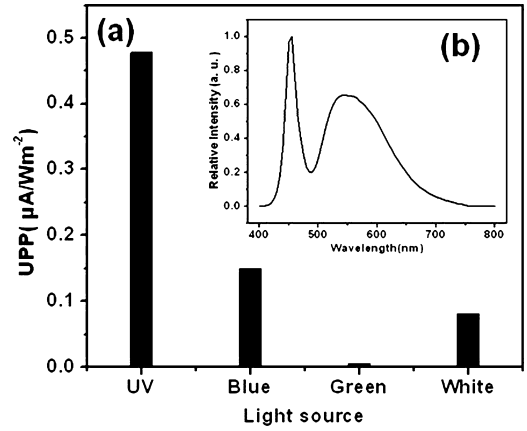

Figure 8. (a) Unit power of photocurrent (UPP) amplitude of device 9 (TiO_2/WO_3 = 2:8) when it was exposed to ultraviolet, blue, green, and white by application to a bias voltage of 0.2 V. (b) The spectral characteristic of white light.

one, which could be ascribed to the high coupling and mixing of TiO_2/WO_3. In this composite system, both TiO_2 and WO_3 are n-type semiconductors, owing to the bottom of conduction band of WO_3 being lower than TiO_2; the electron could transfer easily from TiO_2 to WO_3, which improved the charge separation efficiently. Furthermore, the use of a bias voltage further improved the separation of photogenerated carrier.

From the above results and discussion, therefore, we could conclude that device 9 (TiO_2/WO_3 = 2:8) had the highest photoelectric response in the as-designed material library under the same light source and bias voltage.

3.3. Analysis of the Indistinct Photoelectric Response for TiO_2 and MnO_2 Corners. For these devices of the TiO_2 corner, in the experiment, no distinct photoelectric response was observed under the four kinds of light source; this might be attributed to the small application bias voltage, as the bias voltage of 0.2 V was not sufficient to force electrons to cross the barrier of the grain boundary of TiO_2, which resulted in such a slight response that the obtained photocurrent was small in the circuit. For this possibility, three larger biases, 2, 5, and 10 V were applied to test the photoelectric response for device 1 (pure TiO_2) under ultraviolet irradiation. Figure 9 showed that device 1 had relatively higher response amplitude by applying a bias voltage of 10 V; nevertheless, the obtained photocurrent was comparatively lower at the bias voltage of 2 V. Thus, we might conclude that an obvious photoelectric response would be acquired by applying a larger bias voltage for some composite system; this phenomenon was consistent with the results reported by Pomoni.[31] Here, the application of a larger bias voltage was mainly to enable the electron within the semiconductor across the barrier of the grain boundary between two crystals. However, it would hinder the practical application of the photocatalyst when the bias was too large.

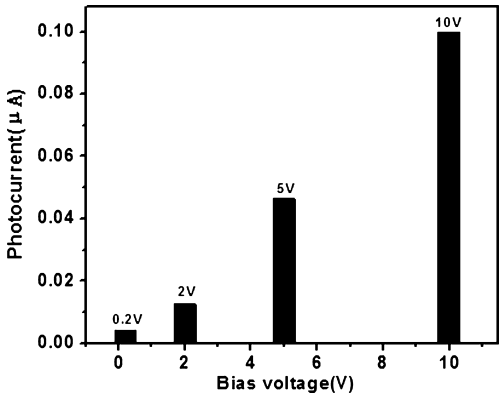

Figure 9. Photoelectric response amplitude of device 1 (pure TiO_2) when it was exposed to ultraviolet light by applying a bias voltage of 0.2, 2, 5, and 10 V, respectively.

For these devices of the MnO_2 corner, similarly, no distinct photoelectric response was observed under any light source or at any bias voltage. As we all know, the manganese was an element whose valence changed with the sintering temperature. Here, the valence of manganese might have changed during the process of sintering. The XRD patterns shown in Figure S1 (Supporting Information) demonstrated that the MnO_2 powder had changed into Mn_2O_3 when it was sintered at 550 °C for 2 h in air. Tanmay et al. prepared Mn_2O_3 doped TiO_2 using TiO_2 and $KMnO_4$, which exhibited photocatalytic activity 3−5 times higher than P25 for oxidation of RB.[32] There were no distinct photoelectric responses at the MnO_2 corner that might attribute to the large amount of Mn_2O_3 of the composite material system in our experiment. Thus, Mn_2O_3 might have a great significance in promoting the separation of electron and hole in TiO_2 when the amount of Mn_2O_3 is less. On the contrary, it might become the recombination center when the amount was too much; the most direct result for it was that the photocurrent in the circuit decreased rapidly.

4. Conclusions

In this study, a material library which was composed of $TiO_2/WO_3/MnO_2$ composite material system was designed. We fabricated 66 devices by means of a ball-milling and screen-printing technique. These processes ensured that all the devices were fabricated under the same conditions. During the overall testing process, a high-throughout screening platform was used, which had greatly improved the efficiency of measurement.

We selected photocurrent as the parameter to evaluate the photoelectrical properties of the semiconductor materials. Through the experiment, we acquired all the photoelectric responses of the 66 composite materials under the same testing conditions. The largest photocurrent was observed when the mole ratio of TiO_2/WO_3 was 2/8 in the composite system, which has great significance for the research of the visible-light-responsive semiconductor for photoelectrocatalysis and photocatalysis.

We expect that the best composite system would have a good efficiency for degradation of organic contaminants under the gas-phase condition using visible light source; the relevant research will be carried out in the near future. At last, we also expect that the method of our experiment will be widely used in the fields of photoelectrocatalysis and photocatalysis for solar energy conversion and environmental purification.

Acknowledgment. This work was supported by the National Basic Research Program of China (Grant Nos. 2009CB939705 and 2009CB939702), Nature Science Foundation of China (No. 50927201), and the Opening Research Foundation of State Key Laboratory of Advanced Technology for Materials Synthesis and Processing (Wuhan University of Technology). The authors are also grateful to Analytical and Testing Center of Huazhong University of Science and Technology.

Supporting Information Available. Figure S1 detailing the phase structure of the powder of device 66 (pure MnO_2). This material is available free of charge via the Internet at http://pubs.acs.org.

References and Notes

(1) Fujishima, A.; Honda, K. *Nature* **1972**, *238*, 37.
(2) Belver, C.; Bellod, R.; Stewart, S. J.; Requejo, F. G.; Fernández-García, M. *Appl. Catal., B* **2006**, *65*, 309–314.
(3) Yang, S. W.; Gao, L. *Mater. Res. Bull.* **2008**, *43*, 1872–1876.
(4) Li, F. B.; Li, X. Z.; Ao, C. H.; Lee, S. C.; Hou, M. F. *Chemosphere* **2005**, *59*, 787–800.
(5) Xiao, G. C.; Wang, X. C.; Li, D. Z.; Fu, X. Z. *J. Photochem. Photobiol., A* **2008**, *193*, 213–221.
(6) Nakanishi, Y.; Imae, T. *J. Colloid Interface Sci.* **2005**, *285*, 158–162.
(7) Inaba, R.; Fukahori, T.; Hamamoto, M.; Ohno, T. *J. Mol. Catal. A* **2006**, *260*, 247–254.
(8) Lo, S. C.; Lin, C. F.; Wu, C. H.; Hsieh, P. H. *J. Hazard. Mater.* **2004**, *114*, 183–190.
(9) Wu, L.; Yu, J. C.; Fu, X. Z. *J. Mol. Catal. A* **2006**, *244*, 25–32.
(10) Ohno, T.; Murakami, N.; Tsubota, T.; Nishimura, H. *Appl. Catal., A* **2008**, *349*, 70–75.
(11) Hamal, D. B.; Klabunde, K. J. *J. Colloid Interface Sci.* **2007**, *311*, 514–522.
(12) Jing, D. W.; Guo, L. J. *Catal. Commun.* **2007**, *8*, 795–799.
(13) Sasikala, R.; Shirole, A.; Sudarsan, V.; Sakuntala, T.; Sudakar, C.; Naik, R.; Bharadwaj, S. R. *Int. J. Hydrogen Energy* **2009**, *34*, 3621–3630.
(14) Wang, Z. Y.; Chen, C.; Wu, F. Q.; Zou, B.; Zhao, M.; Wang, J. X.; Feng, C. H. *J. Hazard. Mater.* **2009**, *164*, 615–620.
(15) Potyrailo, R. A.; Mirsky, V. M. *Chem. Rev.* **2008**, *108*, 770–813.
(16) Jaramillo, T. R.; Baeck, S.-H.; Kleiman-Shwarsctein, A.; Choi, K.-S.; Stucky, G. D.; McFarland, E. W. *J. Comb. Chem.* **2005**, *7*, 264–271.
(17) Sanders, D.; Simon, U. *J. Comb. Chem.* **2007**, *9*, 53–61.
(18) Dai, Q. X.; Xiao, H. Y.; Li, W. S.; Na, Y. Q.; Zhou, X. P. *J. Comb. Chem.* **2005**, *7*, 539–545.
(19) Dai, Q. X.; Xiao, H. Y.; Li, W. S.; Na, Y. Q.; Zhou, X. P. *Appl. Catal., A* **2005**, *290*, 25–35.
(20) Xiao, H. Y.; Dai, Q. X.; Li, W. S.; Au, C. T.; Zhou, X. P. *J. Mol. Catal. A* **2006**, *245*, 17–25.
(21) Chin, S. S.; Chiang, K.; Fane, A. G. *J. Membr. Sci.* **2006**, *275*, 202–211.
(22) Reyes, C.; Fernández, J.; Freer, J.; Mondaca, M. A.; Zaror, C.; Malato, S.; Mansilla, H. D. *J. Photochem. Photobiol., A* **2006**, *184*, 141–146.
(23) Xie, Y. B.; Li, X. Z. *Mater. Chem. Phys.* **2006**, *95*, 39–50.
(24) Liu, B. S.; Wen, L. P.; Zhao, X. J. *Prog. Org. Coat.* **2009**, *64*, 120–123.

(25) Cheng, X. F.; Leng, W. H.; Liu, D. P.; Zhang, J. Q.; Cao, C. N. *Chemosphere* **2007**, *68*, 1976–1984.
(26) Arai, T.; Yanagida, M.; Konishi, Y. *Electrochemistry* **2008**, *76*, 128–131.
(27) Akurati, K. K.; Vital, A.; Dellemann, J.-P.; Michalow, K.; Graule, T.; Ferri, D.; Baiker, A. *Appl. Catal., B* **2008**, *79*, 53–62.
(28) Ke, D. N.; Liu, H. J.; Peng, T. Y.; Liu, X.; Dai, K. *Mater. Lett.* **2008**, *62*, 447–450.
(29) Zhang, L. F.; He, D. P.; Jiang, P. *Catal. Commun.* **2009**, *10*, 1414–1416.
(30) Arai, T.; Konishi, Y.; Iwasaki, Y.; Sugihara, H.; Sayama, K. *J. Comb. Chem.* **2007**, *9*, 574–581.
(31) Pomoni, K.; Vomvas, A.; Trapalis, C. *Thin Solid Films* **2008**, *516*, 1271–1278.
(32) Ghorai, T. K.; Pramanik, S.; Pramanik, P. *Appl. Surf. Sci.* **2009**, *255*, 9026–9031.

CC1000117